3rd Conference on Sustainability in Civil Engineering (CSCE'21)
Department of Civil Engineering
Capital University of Science and Technology, Islamabad Pakistan

PREDICTING THE IMPACT OF CHEMICAL AND PHYSICAL VARIABILITY IN BINARY AND TERNARY CEMENTITIOUS BLENDS

[a] Vireen Limbachiya*, [b] Rabee Shamass,

a: Civil and Building Services Engineering, London South Bank University, limbachv@lsbu.ac.uk
b: Civil and Building Services Engineering, London South Bank University, shamassr@lsbu.ac.uk
* Corresponding author: Email ID: limbachv@lsbu.ac.uk

Abstract- To reduce the quantity of CO_2 emitted within the construction industry, cementitious by-products will need to be implemented on a larger scale. In relation to the use of by-products, one of the biggest disadvantages is that not only from source to source, obtaining a by-product from the same source could result in a variation in the chemical and physical properties which will then impact the mechanical properties. Therefore, the paper reviewed binary and ternary cementitious pastes that were produced from 7 different by-products and predicted the impact of variation in the chemical and physical properties on the 14-day compressive strength. The predictions and analysis were done with the use of artificial neural networks (ANN). Overall, ANN successfully derived an accurate prediction which correlated with the trends that were expected. This study noted that if parameters of the overall mix were taken into consideration, the increase in SiO_2 will have a negative impact while increase in CaO would have a positive impact on the 14-day strength. The most accurate form of understanding the impact of chemical and physical variability of cementitious replacements, took into consideration both Ca/Si ratio and the average particle size.

Keywords- ANN, Cement Replacements, Predicting Compressive Strength, Binary and Ternary Cementitious Pastes.

1 Introduction

Studies have reviewed many combinations of cementitious by-products that can be used as an alternative for Ordinary Portland Cement (OPC) [1,2]. The impact of Pulverised Fuel Ash (PFA) and By-Pass Dust (BPD) obtained over a 6-month period from the same source was analysed by Limbachiya et al [3]. The results showed a clear variation in the chemical and physical properties and the correlating impact on strength development. Shi et al. [4] reported on four different forms of glass powder being used as a cementitious replacement. They noted that the particle size has a large effect on the compressive strength of concrete, as replacements containing larger particles size produced lower strengths at 28 days. Overall results showed one of the biggest disadvantages of using by-products is that not only from source to source, obtaining a by-product from the same source could result in a variation in the chemical and physical properties, which thereafter will result in a variation in concrete strength.

When there is variation in OPC, Bogues equations are used to predict the quantity of compounds that will be produced during the hydration process and therefore, an indication of strength development. Bogues equations use the oxide composition of OPC to determine the level of alite, belite, tricalcium aluminate and tetracalcium aluminoferrite [5], which are responsible for different properties within concrete. As well as the individual oxide values, oxide ratios are known to help predict the behaviour of concrete. In a review of the influence of the Ca/Si ratio on the compressive strength of cementitious calcium–silicate–hydrate binders, it was concluded that as Ca/Si ratio decreases the compressive strength increase [6]. It was reported that the diffraction peaks' intensity of calcite became stronger as the Al/Si ratio decreases [7]. It is assumed that as the Al/Si ratio increases the calcite decreases, therefore, greater formation of strength gaining compounds. Finally, it was concluded that for lower ratios of Mg/Si, unreacted silica remained and for higher ratios brucite precipitated. Therefore, greater forms of deterioration are likely to occur at higher ratio levels [8].

When it comes to a variation of properties in cement replacements, there are no such tools that can be used to help understand the impact on strength development. Studies have used artificial neural networks (ANN) to predict the strength of concrete using more sustainable materials. ANN was used to understand the effect of Nano and Micro Silica on the compressive and flexural strength of cement mortar [9]. The variables in this case were the quantity of different components used in the mortar mixture. The study concluded that the ANN model was able to predict the compressive strength to a high level of accuracy. Alongside ANN, Fuzzy Logic (FL) models have been used by previous studies to help predict the behaviour of concrete [10,11]. Although both models can provide high levels of accuracy, both studies concluded that ANN provided a greater level of statistical accuracy in comparison to FL. Currently, there are very few studies that have looked at a range of chemical and physical variations in by-product combinations and the impact of this on the strength of cementitious mixes consisting of binary and ternary blends. Therefore, the aim of this study is to use ANN to predict the impact of chemical and physical variability in cementitious by-products. The objectives are to firstly, produce ternary and binary cementitious pastes. Secondly, use the chemical and physical properties of these mixes as input parameters to help predict and determine the parameters that have an impact on the compressive strength. The significance of this work is that it will allow for a better understanding on the impact of chemical and physical variability when using binary and ternary cementitious pastes and determine how ANN can be used to help predict this behaviour.

2 Research Methodology

2.1 Cementitious materials

The OPC fulfilled the requirements of BS EN 197-1 CEM I [12]. The cementitious materials used in this study were obtained from a variety of sources. Ground Granulated Blast Furnace Slag (GGBS), (PFA), Metakaolin (MK), BPD and Silica Fume (SF) came in powder form to be used within the cementitious binders, while Basic Oxygen Slag (BOS) and Glass Powder (GP) came in a crushed form and required further grinding before adequate levels of fineness were achieved. Table 1 provides the physical and chemical properties using of Hydro 2000/Mastersizer 2000 and X-Ray Fluorescence (XRF) respectively.

Table 1 Chemical and physical properties of OPC and Cement Replacements.

Composition	SiO_2 (%)	TiO_2 (%)	$Al2O_3$ (%)	Fe_2O_3 (%)	MnO (%)	MgO (%)	CaO (%)	Na_2O (%)	K_2O (%)	P_2O_5 (%)	SO_3 (%)	Average Particle Size (µm)
OPC	19.42	0.36	4.55	2.49	0.02	1.03	60.60	0.22	0.57	0.2	3.62	38
PFA	45.85-52.29	0.98-0.82	24.43-19.76	10.38-7.55	0.16-0.06	2.09-1.44	6.13-2.81	0.91-0.63	2.75-2.02	0.51-0.22	0.84-0.48	55-32
GGBS	33.28	0.57	13.12	0.32	0.32	7.74	37.16	0.33	0.48	0.01	2.21	20
SF	94.21	0.01	0.48	0.71	0.01	0.55	0.37	0.35	1.15	0.04	0.17	0.7
BOS	13.94	0.7	2.98	25.99	3.17	6.56	39.57	0.06	0.03	1.51	0.28	30
GP	69.56	0.07	2.01	0.65	0.32	1.19	10.61	12.28	0.98	0.03	0.18	100
MK	54.06	0.02	40.65	0.77	0.01	0.23	0.03	0.17	1.89	0.16	0.02	7
BPD	17.34-12.79	0.23-0.19	4.26-3.47	2.36-1.88	0.05-0.04	1.11-0.82	53.6-44.03	1.16-0.5	10.06-4.28	0.25-0.12	12.22-6.25	67-32

2.1 Mix Design and Fabrication

130 cementitious pastes were produced, tested, and analysed by the author in the laboratory for this study. All cementitious pastes were produced as a semi dry mix with constant w/c ratio of 0.2, therefore the variability in the results could only be due to the difference in the chemical and physical properties of the materials used. To produce samples, the binary//ternary

mixtures were mixed thoroughly before water was added and compaction was applied. Thereafter, the samples were cured and tested following guidance in BS EN1338:2003. The paste cubes had a dimension of 50x50x50mm, and the compressive strength was obtained at 14 days. The mixes produced had varying levels of OPC and by products. OPC, PFA, BPD, GGBS, GP, SF, BOS and MK was used to produce the cement pastes by up to 60%, 80%,10%, 80%, 15%, 15%, 45% and 30% by weight respectively. All mixes can be found in Appendix A.

3. Artificial Neural Network setup

3.1 Input and target parameters

Input properties were based on the combined oxide properties of ternary and binary mixes, which were obtained by using Equation 1 that was developed for this study. Table 2 provides the actual oxide compositions determined using XRF for 11 ternary and binary mixes, as well as the predicted oxide compositions using Equation 1. Based on these results, Equation 1 was determined to provide an accurate assumption on the combined oxide percentage and therefore be used in the ANN models.

$$\mathrm{Input_n} = \left(\frac{\%\mathrm{OPC}}{100} * \mathrm{OPC_n}\right) + \left(\frac{\%\mathrm{CR1}}{100} * \mathrm{CR1_n}\right) + \left(\frac{\%\mathrm{CR2}}{100} * \mathrm{CR2_n}\right) \qquad \textit{(Equation 1)}$$

Where $\mathrm{Input_n}$ is the input parameter for the ANN model, %OPC is the percentage of OPC used in the mix, n represents the chemical or physical property, $\mathrm{OPC_n}$ is the quantity of n in OPC, %CR1 and %CR2 are the percentages of cement replacements used in the mix and $\mathrm{CR1_n}$ and $\mathrm{CR2_n}$ are the quantity of n in the cement replacement.

Table 2 Accuracy of Predicted Ternary and Binary oxides

	SiO_2 (%)		CaO (%)		Al_2O_3 (%)		Fe_2O_3 (%)	
Mix	Actual	Predicted	Actual	Predicted	Actual	Predicted	Actual	Predicted
1	24.53	24.96	50.49	51.22	6.73	7.98	1.69	1.62
2	31.25	32.22	45.57	45.91	5.16	5.76	1.74	1.69
3	20.62	21.10	50.27	51.71	5.33	5.95	6.31	6.76
4	23.42	24.14	50.96	52.05	6.40	7.53	1.77	1.72
5	23.96	24.71	49.23	50.52	6.69	7.94	1.64	1.61
6	16.51	17.23	51.21	52.19	3.64	3.92	11.18	11.89
7	27.98	30.75	38.42	37.66	10.19	12.38	4.65	5.58
8	35.49	37.72	37.62	37.23	7.55	8.83	3.60	4.16
9	33.91	34.10	44.82	45.71	5.76	6.08	1.56	1.68
10	31.60	31.06	46.25	47.55	5.72	6.71	1.63	1.66
11	28.94	29.53	48.75	48.46	5.94	7.03	1.70	1.65

3.2 Neural Network setup.

Figures 1 and 2 show the ANN models developed in this study, namely NN 5-7 and NN 4-7. Seven neurons in the hidden layer were chosen as they provided accurate predictions. The five input parameters for NN 5-7 were based on the combined chemical properties that form alite, belite, tricalcium aluminate and tetracalcium aluminoferrite, as well as the average particle size. The four input parameters for NN 4-7 were ratios that are known to have a direct impact on hydration compounds and formation of calcium silicate hydrate (CSH) as well as the average particle size.

To have a more effective ANN setup, the input and target parameters are normalised [13]. The calculated output will then also provide a normalised value, which will require it to be reverse transformed to obtain the actual target value. To normalize the input and output parameters, Equation 2 was applied to all values. Where a_{min} and a_{max} are constants, b_{max} is the greatest value of that parameter, b_{min} is the lowest value of that parameter, b is the actual value and a is the normalised value. Table 3 provides the values required to de-normalise the values.

$$a = (a_{max}-a_{min})*(b-b_{min})/(b_{max}-b_{min}) + a_{min} \qquad \textit{(Equation 2)}$$

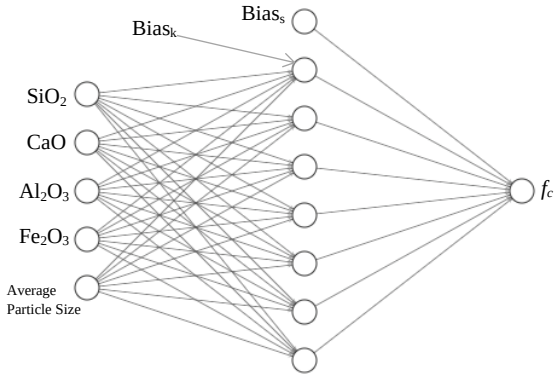

Figure 1 NN 5-7 Model

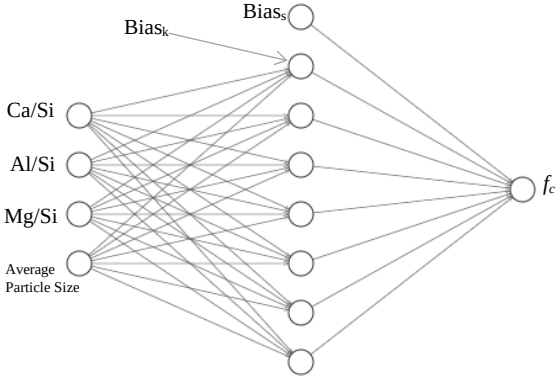

Figure 2 NN 4-7Model.

Table 3 Parameters used to normalise input and target values

Input/Target Parameter	a_{max}	a_{min}	b_{min}	b_{max}
SiO_2	1	-1	16.12	53.30
CaO	1	-1	5.69	60.23
Al_2O_3	1	-1	3.61	26.34
Fe_2O_3	1	-1	0.49	16.59
Ca/Si	1	-1	0.11	3.15
Al/Si	1	-1	0.18	0.58
Mg/Si	1	-1	0.02	0.28
Average Particle Size (µm)	1	-1	18.01	58.9
f_c(MPa)	1	-1	0	70.40

Once the input and output parameters were determined, the next step was to define the neural network. A pre-installed neural network fitting app in Matlab was used in this study. The neural network fitting app solves an input-output fitting problem with a two-layer feedforward neural network. The network was a two-layer feed-forward network with sigmoid hidden neurons and linear output neurons and trained with Levenberg-Marquardt backpropagation algorithm, unless there is not enough memory, in which case scaled conjugate gradient backpropagation will be used [13]. The backpropagation algorithm involves two phases. Firstly, the forward phase where the activations are propagated from the input to the output layer [11]. Secondly, the backward phase where the error between the observed actual value and the desired nominal value in the output layer is propagated backwards to modify the weights and bias values [11]. Equations 3 and 4 provide the calculations that includes the transfer function required to determine the normalised target value based on the inputs provided [14]. Where, O_s is the normalised ouput value, q is the number of input parameters; r is the number of hidden neurons; s is the number of output parameters; $Bias_s$ and $Bias_k$ are the biases of s^{th} output neuron and kth hidden neuron (H_k), respectively; with j,k is the weights of the connection between I_j and are the weights of the connection between H_k and O_s

$$O_s = Bias_s + \sum_{k=1}^{r} w_{k,l}^{ho} \cdot \frac{2}{(1+e^{(-2\,x\,H_k)})-1} \qquad \textit{(Equation 3)}$$

$$H_k = Bias_k + \sum_{j=1}^{q} w_{j,k}^{ih} . I_j \qquad \textit{(Equation 4)}$$

For training, validation and testing the data sets were divided into 70%, 15% and 15% respectively. To assess the accuracy of the output the regression (R^2), Root Mean Square Error (RMSE), Mean Absolute Percentage Error (MAPE) and Mean Square Error (MSE) were calculated using equations 5, 6, 7 and 8 respectively.

$$R^2 = 1 - \left(\frac{\sum_{i=1}^{N}(ti-Oi)^2}{\sum_{i=1}^{N}(ti-tm)^2}\right) \quad \textit{(Equation 5)}$$

$$RMSE = \sqrt{\frac{\sum_{i=1}^{N}(Oi-ti)^2}{N}} \quad \textit{(Equation 6)}$$

$$MAPE = \frac{1}{N}\sum_{i=1}^{N}\left|\frac{Oi-ti}{ti}\right| \times 100 \quad \textit{(Equation 7)}$$

$$MSE = \frac{\sum_{i=1}^{N}(Oi-ti)^2}{N} \quad \textit{(Equation 8)}$$

Where t_i is the actual compressive strength of concrete mixes, t_m is the mean compressive strength of concrete mixes, O_i is the predicted value and N is the total number of data points in each set of data.

3.3 Impact of Individual Input

As well as assessing the accuracy of the models with Equations 5 and 6, it is also important to understand the impact of input parameters on the output value. This will allow for further validation of the ANN model and algorithms, as it will have the potential to be used for values outside of those used in this model. It is important to note that the values will still have to remain within the ranges stated in Table 3. To determine the impact of each input parameter, the connection weight approach was adopted. The connection weight approach uses raw connection weights, which accounts for the direction of the input–hidden–output relationship and results in the correct identification of variable contribution [15]. Based on this approach, Equation 9 was used to determine impact of each input parameter. A negative value will mean that an increase in this parameter will decrease the output value, a positive value will mean that an increase in this parameter will increase the output value and those values with the largest value are those with the largest impact.

$$Input_x = \sum_{Y=A}^{E} Hidden_{XY} \quad \text{(Equation 9)}$$

3 Results

3.1 Predicting the impact of chemical and physical variability

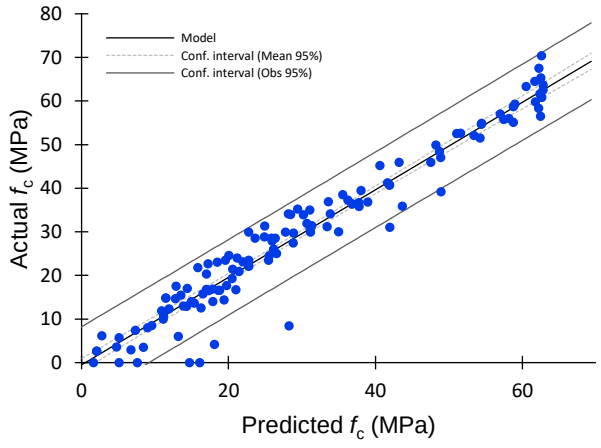

Figure 3 Regression of Actual fc vs predicted fc for NN 5-7

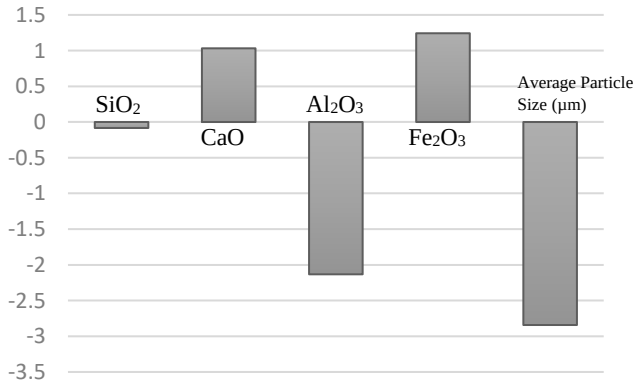

Figure 4 Influence of each input for NN 5-7

$$f_c = -0.84 - 1.47\left(\frac{2}{(1+e^{(-2H_1)})}-1\right) - 0.29\left(\frac{2}{(1+e^{(-2H_2)})}-1\right) - 0.74\left(\frac{2}{(1+e^{(-2H_3)})}-1\right) + 1.86\left(\frac{2}{(1+e^{(-2H_4)})}-1\right) - 1.89\left(\frac{2}{(1+e^{(-2H_5)})}-1\right) - 0.25\left(\frac{2}{(1+e^{(-2H_6)})}-1\right) + 0.55\left(\frac{2}{(1+e^{(-2H_7)})}-1\right)$$

(Equation 10)

Where:
H_1= -1.80 + 0.29SiO_2 + 0.20CaO + 1.90 Al_2O_3- 4.06Fe_2O_3 + 1.49 Average Particle Size (µm)
H_2= 1.97 + 0.52SiO_2 – 1.01CaO + 2.29Al_2O_3 + 0.15Fe_2O_3 -0.63 Average Particle Size (µm)
H_3= -0.03 + 1.22SiO_2 - 0.71CaO – 2.74Al_2O_3 + 0.22Fe_2O_3 – 1.19 Average Particle Size (µm)
H_4= -0.87 + 0.25SiO_2 + 0.43CaO + 1.68Al_2O_3 – 2.27Fe_2O_3 + 0.35 Average Particle Size (µm)
H_5= 1.08 – 0.42SiO_2 + 0.23CaO + 1.96Al_2O_3 - 0.38Fe_2O_3 – 0.42 Average Particle Size (µm)
H_6= 1.84 + 2.71SiO_2 – 4.00CaO + 0.46Al_2O_3 – 1.37Fe_2O_3+ 3.03 Average Particle Size (µm)
H_7= -2.42 + 1.47SiO_2 – 1.56CaO – 0.07Al_2O_3 – 2.45Fe_2O_3 – 4.36 Average Particle Size (µm)

Figure 3 provides the predicted vs experimental strengths for the NN 5-7 model. Equation 10 is derived from algorithms used in the ANN model for predicting the 14-day compressive strength. The R^2, RMSE, MSE and MAPE values were 0.95,4.36, 18.98 and 17.97, respectively. Overall, the results show that ANN can predict compressive strength to a high level of accuracy when oxide values are considered using Equation 1. It is assumed that the accuracy is closely related to the input parameters behaving in the way that is expected. Figure 4 provides the impact that each input parameter has on the output value. Results show that as SiO_2, Al_2O_3 and Average particle size increases, there will be a negative impact on the output and that as CaO and Fe_2O_3 increases, there is a positive impact on the output. Studies [16][17][18] have previously noted that cement replacements with a high SiO_2 content provide greater strength development through secondary reaction with Ca $(OH)_2$. However, when SiO_2 is determined using Equation 1, results show that overall, as SiO_2 increases the strengths tend to decrease and that as CaO increases there is an increase in strength. This therefore correlates with result that you would expect to occur in OPC hydration in which the ratio of Ca/Si dictates the formation of compounds and therefore strength development. Fe_2O_3 is the input that is responsible for the greatest strength gain. Although studies [19] have reported on the positive impact of Nano Fe_2O_3 on the compressive strength of concrete, the strength development in concrete is primarily down to the formation of Calcium silicate (Ca_3SiO_5) and Larnite (Ca_2SiO_4). Overall, the biggest impact on strength development was the average particle size. Results show that as average particle size increases the strength decreases. This correlated with conclusions made is previous studies [4] and is assumed to be due to the water not being able to react with the oxides within the inner particle of the material.

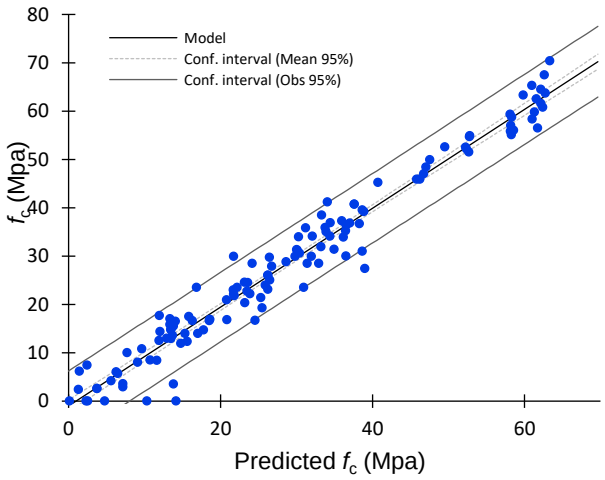

Figure 5 Regression of Actual fc (MPa) vs predicted fc (MPa) for NN 4-7

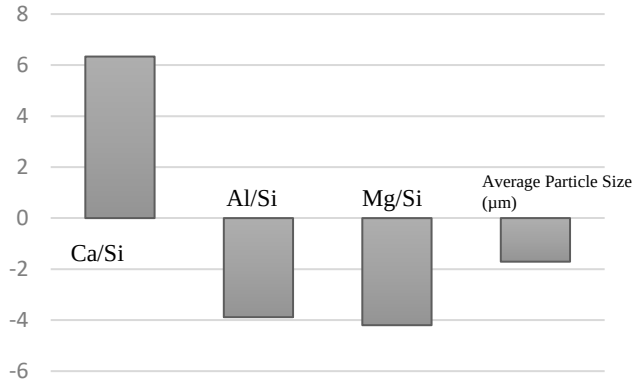

Figure 6 Influence of each input for NN 5-7-1

$$f_c = 1.04 + 0.67\left(\frac{2}{(1+e^{(-2H_1)})}-1\right) + 0.38\left(\frac{2}{(1+e^{(-2H_2)})}-1\right) - 0.36\left(\frac{2}{(1+e^{(-2H_3)})}-1\right) + 0.64\left(\frac{2}{(1+e^{(-2H_4)})}-1\right) + 0.73\left(\frac{2}{(1+e^{(-2H_5)})}-1\right) + 1.72\left(\frac{2}{(1+e^{(-2H_6)})}-1\right) + 1.00\left(\frac{2}{(1+e^{(-2H_7)})}-1\right)$$

(Equation 11)

Where:
H_1= 1.79 + 0.34Ca/Si – 1.79Al/Si - 1.86 Mg/Si – 0.29 Average Particle Size (µm)
H_2= 1.20 – 0.43Ca/Si – 2.36Al/Si – 0.26 Mg/Si – 0.15 Average Particle Size (µm)
H_3= 0.31 – 0.66Ca/Si + 2.31Al/Si + 2.17 Mg/Si + 3.15 Average Particle Size (µm)
H_4=0.02 – 1.16a/Si + 0.12Al/Si + 1.10 Mg/Si + 1.41 Average Particle Size (µm)
H_5= -0.74 + 0.89Ca/Si + 1.92Al/Si + 0.37 Mg/Si – 0.64 Average Particle Size (µm)
H_6=1.76 + 2.61Ca/Si + 0.08Al/Si - 1.77 Mg/Si – 0.18 Average Particle Size (µm)
H_7= 3.96 – 1.50Ca/Si – 1.67Al/Si + 1.43 Mg/Si + 0.26 Average Particle Size (µm)

Figure 5 provides the predicted vs experimental strengths for the NN 4-7 model. Equation 11 is derived from algorithms used in the ANN model for predicting the 14-day compressive strengths. The R^2, RMSE, MSE and MAPE values are 0.96,3.61, 13.05 and 14.92, respectively. In comparison to oxide percentages, oxide ratios predict output with a higher level of accuracy and a greater level of confidence. It is assumed R^2, RMSE, MSE and MAPE provide a greater level of accuracy as the ratios correlate to the formation of compounds that are responsible for strength development. Therefore, ANN can correlate more accurately with the output parameter. Figure 6 shows that the only ratio that contributes to strength development is Ca/Si, while Al/Si, Mg/Si and average particle size all have a negative impact. Overall, these results show that when taking into consideration the combined oxide values, the trends follow those that are noted for OPC hydration. Alite has a Ca/Si ratio of 3:1 and C-S-H has a Ca/Si ratio of approximately 2:1, so excess lime is available to produce $Ca(OH)_2$ [20]. Alite is responsible for early age strength development as well as formation of $Ca(OH)_2$ and results show that as Ca/Si increases, the trend is that strength properties will also increase. When reviewing Al/Si, trends show a decrease in strength as the ratio increases. This correlates with the results that were obtained, in which it was concluded that depending on the Al_2O_3/SiO_2 ratio, the ye'elimite and gehlenitephases were formed in different proportions [21]. It is therefore assumed that in the mixes reviewed, at lower ratios of Al/Si, content of gehlenite exceeds the ye'elimite content therefore decreasing strength properties.

4 Conclusion

The overall the aim of this study was to produce an ANN system that can be used to predict the compressive strength of cement paste at 14 days and to help in gaining a better understanding of the chemical and physical properties of by-products that impact strength. Based on the report the following conclusions can be made:

- Cementitious replacements for OPC come from a variety of sources with varying chemical and physical properties. Based on the level of replacement, the use of these materials will have an impact on the hydration compounds produced and therefore, strength.
- Although previous studies have noted that a high SiO_2 content in the cement replacement would allow for an enhancement in strength with secondary hydration of $Ca(OH)_2$. This study noted that if parameters of the overall mix as shown in Equation 1 were taken into consideration, the increase in SiO_2 will have a negative impact on strength.
- When reviewing oxide values, oxide ratios provided the most accurate trendlines. Results showed when taking all parameters in consideration, the trend was like that of OPC hydration alone, in which Ca/Si determined the early age strength.
- Overall, results showed that the most accurate form of understanding the impact that chemical and physical variability of cementitious replacements would have, took into consideration both Ca/Si and the average particle size.
- ANN is a powerful tool in helping us gain a better understanding of the impact that each input has in relation to the target and allowing accurate prediction of the strength of concrete which incorporates cement replacements.
- ANN was successfully used in this study to provide an accurate prediction which correlated with the trends that were noted in the oxide analysis.

Acknowledgment

The authors gratefully appreciate and acknowledge the financial support from the 2 Engineering and Physical Sciences Research Council who had sponsored the PhD programme. The authors also acknowledge the support and facilities that were provided at Coventry University and London South Bank University.

References

[1] Qureshi, L., Ali, B. and Ali, A. (2020). Combined effects of supplementary cementitious materials (silica fume, GGBS, fly ash and rice husk ash) and steel fiber on the hardened properties of recycled aggregate concrete, Construction and Building Materials, 263, 120636.

[2] Gehlot, T., Sankhla, S. and Parihar, S. (2021). Modelling compressive strength, flexural strength and chloride ion permeability of high strength concrete incorporating metakaolin and fly ash. Materials Today Proceedings, in press.

[3] Limbachiya, V., Ganjian, E. and Claisse, P. (2015). The impact of variation in chemical and physical properties of PFA and BPD semi-dry cement paste on strength properties, Construction and Building Materials, 96, pp. 248-255

[4] Shi, C., Wu, Y., Riefler, C., and Wang, H. (2005). Characteristics and Pozzolanic Reactivity of Glass Powders. Cement and Concrete Research, 35 (5),pp. 987-993

[5] Neville, A. (1996) Properties of Concrete. Fourth Edition, Wiley.

[6] Kunthur, W., Ferreiro, S. and Skibsted,J. (2017). Influence of the Ca/Si ratio on the compressive strength of cementitious calcium–silicate–hydrate binders, Journal of Materials Chemistry A, 5, pp. 17401-17412.

[7] Li, J., Yu, Q., Huang, H. and Yin, s. (2019). Effects of Ca/Si Ratio, Aluminum and Magnesium on the Carbonation Behavior of Calcium Silicate Hydrate, Materials. 12, 1268.

[8] Nied, D., Enemark-Rasmussen, K., L'Hopital, E., Skibsted, J., & Lothenbach, B. (2016). Properties of magnesium silicate hydrates (M-S- H). Cement and Concrete Research, 79, pp. 323-332

[9]] Azimi-Pour, M. and Eskandari-Naddaf, H. (2018) ANN and GEP prediction for simultaneous effect of nano and micro silica on the compressive and flexural strength of cement mortar, Construction and Building Materials, 189 , pp. 978-992.

[10] Ozcan, F., Atis, C., Karahan, O., Uncuoglu, E. and Tanyildizi, H. (2009). Comparison of artificial neural network and fuzzy logic models for prediction of long-term compressive strength of silica fume concrete. Advances in Engineering Software, 40 (9), pp.856-863.

[11] Golafshani, E.M., Rahai, A., Sebt, M.H. and Akbarpour, H. (2012). Prediction of bond strength of spliced steel bars in concrete using artificial neural network and fuzzy logic. Construction and Building Materials, 36, pp.411-418.

[12] British Standard Institution, BS EN 197-1 Cement Composition, specifications and conformity criteria for common cements BSI, London (2011)

[13] MATLAB and Statistics Toolbox Release 2019a, The MathWorks, Inc., Natick, Massachusetts, United States.

[14] Gupta, T., Patel, K. A., Siddique, S., Sharma, R. K. and Chaudhary, S. (2019) Prediction of mechanical properties of rubberised concrete exposed to elevated temperature using ANN, Measurement, 147, pp. 106870.

[15] Olden, J. D., Joy, M. K. and Death, R. G. (2004) An accurate comparison of methods for quantifying variable importance in artificial neural networks using simulated data, Ecological Modelling, 178 (3), pp. 389-397.

[16] Behnood, A. and Ziari, H. (2008). Effects of Silica Fume Addition and Water to Cement Ratio on the Properties of High-Strength Concrete After Exposure to High Temperatures. Cement and Concrete Composites 30 (2), 106-112

[17] Papadakis, V. G. (1999) Effect of Fly Ash on Portland Cement Systems: Part I. Low- Calcium Fly Ash. Cement and Concrete Research ,29 (11), 1727-1736

[18] Köksal, F., Altun, F., Yiğit, İ., and Şahin, Y. (2008) Combined Effect of Silica Fume and Steel Fiber on the Mechanical Properties of High Strength Concretes. Construction and Building Materials 22 (8), 1874-1880

[19] Zhang, A., Ge, A., Yang, W., Cai, X. and Du, Y. (2019). Comparative study on the effects of nano-SiO2, nano-Fe2O3 and nano-NiO on hydration and microscopic properties of white cement. Construction and Building Materials, 228 ,116767.

[20] Winter, N. (2012). Understanding Cement. Woodbridge: WHD Microanalysis Consultants Ltd.

[21] Berrio, A., Rodriguez, C. and Tobon, J. (2018). Effect of Al2O3/SiO2 ratio on ye'elimite production on CSA cement. Construction and Building Materials, 168, pp.512-521.

Appendix A

1	OPC20/PFA80*	44	OPC20.63/PFA68.12/SF11.25	87	OPC5/GGBS60/BOS25
2	PFA80/MK20	45	OPC5/PFA80/SF15	88	OPC30/GGBS40/BOS30
3	OPC14/PFA56MK30	46	OPC12.5/PFA80/SF7.5	89	OPC35/GGBS20/BOS45
4	OPC14/PFA66/MK20	47	OPC60/PFA25/SF15	90	OPC45/GGBS40/BOS15
5	OPC24/PFA66/MK10	48	OPC48.13/PFA48.12/SF7.5	91	OPC45/GGBS20/BOS35
6	OPC44/PFA26/MK30	49	OPC60/PFA32.5/SF7.5	92	OPC25/GGBS60/BOS15
7	OPC60/PFA40	50	OPC28.13/PFA68.12/SF3.75	93	OPC15/GGBS40/BOS45
8	OPC60/MK40	51	OPC36.25/PFA56.25/SF7.5	94	GGBS40/BOS60
9	OPC27/PFA46/MK10	52	OPC15/PFA80/SF5	95	GGBS60/BOS40
10	OPC28/PFA52/MK20	53	OPC48.13/PFA40.62/SF11.25	96	OPC47.5/PFA47.5/GP5
11	OPC60/GGBS40	54	OPC20.63/GGBS68.12/SF11.25	97	OPC30/PFA50/GP20
12	OPC14/GGBS56/MK30	55	OPC5/GGBS80/SF15	98	OPC27.5/PFA67.5/GP5
13	OPC14/GGBS66/MK20	56	OPC12.5/GGBS80/SF7.5	99	OPC47.5/PFA37.5//GP15
14	OPC44/GGBS46/MK10	57	OPC60/GGBS25/SF15	100	OPC35/PFA55/GP10
15	OPC28/GGBS52/MK20	58	OPC48.13/GGBS48.12/SF7.5	101	OPC60/PFA20/GP20
16	OPC24/GGBS66/MK10	59	OPC60/GGBS32.5/SF7.5	102	OPC10/PFA80/GP10
17	OPC44/GGBS26/MK30	60	OPC28.13/GGBS68.12/SF3.75	103	OPC17.5/PFA67.5/GP15
18	OPC20/GGBS80	61	OPC36.25/GGBS56.25/SF7.5	104	OPC60/PFA30/GP10
19	OPC37.5/PFA57.5/BPD5	62	OPC48.13/GGBS40.62/SF11.25	105	OPC47.5/GGBS47.5/GP5
20	OPC23.75/PFA68.75/BPD2.5	63	OPC43/PFA38/GGBS19	106	OPC30/GGBS50/GP20
21	OPC28.75/PFA68.75/BPD25	64	OPC24/PFA58/GGBS18	107	OPC27.5/GGBS67.5/GP5
22	OPC15/PFA80/BPD5	65	OPC24/PFA18/GGBS58	108	OPC47.5/GGBS37.5//GP15
23	OPC60/PFA30/BPD10	66	OPC14/PFA28/GGBS58	109	OPC35/GGBS55/GP10
24	OPC48.75/PFA48.75/BPD2.5	67	OPC26/PFA37/GGBS37	110	OPC40/GGBS60
25	OPC60/PFA35/BPD5	68	OPC14/PFA58/GGBS28	111	OPC60/GGBS20/GP20
26	OPC10/PFA80/BPD10	69	OPC44/PFA18/GGBS38	112	OPC10/GGBS80/GP10
27	OPC48.75/PFA43.75/BPD7.5	70	OPC5/PFA60/BOS25	113	OPC17.5/GGBS67.5/GP15
28	OPC37.5/GGBS57.5/BPD5	71	OPC30/PFA40/BOS30	114	OPC60/GGBS30/GP10

29	OPC23.75/GGBS68.75/BPD2.5	72	OPC35/PFA20/BOS45	115	OPC90/PFA-JUL10*
30	OPC28.75/GGBS68.75/BPD25	73	OPC45/PFA40/BOS15	116	OPC90/PFA-AUG10*
31	OPC15/GGBS80/BPD5	74	OPC45/PFA20/BOS35	117	OPC90/PFA-SEP10*
32	OPC60/GGBS30/BPD10	75	OPC40/BOS60	118	OPC90/PFA-OCT10*
33	OPC48.75/GGBS48.75/BPD2.5	76	OPC25/PFA60/BOS15	119	OPC90/PFA-NOV10*
34	OPC60/GGBS35/BPD5	77	OPC15/PFA40/BOS45	120	OPC90/PFA-DEC10*
35	OPC10/GGBS80/BPD10	78	OPC60/BOS40	121	OPC80/PFA-JUL20*
36	OPC48.75/GGBS43.75/BPD7.5	79	OPC40/PFA60	122	OPC80/PFA-AUG20*
37	OPC70/PFA-NOV30*	80	OPC90/BPD-JUL10*	123	OPC80/PFA-SEP20*
38	OPC70/PFA-DEC30*	81	OPC90/BPD-AUG10*	124	OPC80/PFA-OCT20*
39	OPC95/BPD-JUL5*	82	OPC90/BPD-SEP10*	125	OPC80/PFA-NOV20*
40	OPC95/BPD-AUG5*	83	OPC90/BPD-OCT10*	126	OPC80/PFA-DEC20*
41	OPC95/BPD-SEP5*	84	OPC90/BPD-NOV10*	127	OPC70/PFA-JUL30*
42	OPC95/BPD-OCT5*	85	OPC90/BPD-DEC10*	128	OPC70/PFA-AUG30*
43	OPC95/BPD-NOV5*	86	OPC95/BPD-DEC5*	129	OPC70/PFA-SEP30*
				130	OPC70/PFA-OCT30*

*OPC20/PFA80- 20%OPC and 80%PFA in the cementitious paste